PROCEEDINGS OF SCIENCE

Status of the Double Chooz experiment

Matthieu Vivier*
CEA-Saclay
E-mail: matthieu.vivier@cea.fr

The Double Chooz reactor antineutrino experiment aims for a precision measurement of the neutrino mixing angle θ_{13}, by measuring an energy-dependent deficit in the detected antineutrino spectrum. Double Chooz is located at the Chooz nuclear power plant in France, and has recently finished taking data with a single far detector filled with gadolinium-loaded liquid scintillator at a baseline of 1.05 km. A second identical detector, located at an average distance of 400 m from the two reactor cores has been commissioned and is now operated simultaneously to the far detector. In this article, an overview of the current status of the experiment is given. The physics motivations and the working principle of the detectors are briefly reviewed. A rate + shape fit to the energy spectrum of the antineutrinos detected with a 467.90 days live time dataset accumulated in the far detector yields $\sin^2(2\theta_{13}) = 0.090^{+0.032}_{-0.029}$. Different methods, each sensitive to different systematics, have been used by the collaboration to assess the robustness of this result and are explained here. A deviation from the reactor flux predictions above a visible energy of 4 MeV, which does not affect the $\sin^2(2\theta_{13})$ measurement, is also reported and briefly discussed.

16th International Workshop on Neutrino Factories and Future Neutrino Beam Facilities
25 -30 August, 2014
University of Glasgow, United Kingdom

*Speaker.

PoS(NUFACT2014)041

1. Introduction

Neutrino oscillations have been observed in solar, atmospheric, long baseline accelerator and reactor neutrino experiments [1]. The data collected so far by these experiments are well-described in the framework of a three active neutrino oscillation picture, in which the three known flavor neutrinos (ν_e, ν_μ, ν_τ) are unitary linear combinations of three mass states (ν_1, ν_2, ν_3) with well measured squared mass differences and mixing angles [1], but a yet unknown CP-violating phase. The θ_{13} mixing angle was the last to be measured by short baseline reactor and long baseline accelerator experiments [2, 3, 4, 5, 6, 7, 8, 9]. For MeV neutrino energies, and km-scale baselines, as for example relevant to reactor experiments such as Double Chooz (DC), the $\bar{\nu}_e$ survival probability is well approximated by:

$$P_{\bar{\nu}_e \to \bar{\nu}_e} = 1 - \sin^2(2\theta_{13}) \sin^2\left(1.27 \frac{\Delta m^2_{31}[eV^2]L[m]}{E[MeV]}\right), \tag{1.1}$$

where L is the reactor-detector distance and E the $\bar{\nu}_e$ energy. From equation (1.1), it can be seen that $\bar{\nu}_e$ oscillations both lead to a rate deficit and a distortion of the energy spectrum. Both these information can be used to infer the θ_{13} mixing angle, and is called "rate + shape" analysis. The latest DC measurement [7] assumes $\Delta m^2_{31} = 2.44^{+0.09}_{-0.10} \times 10^{-3}\,eV^2$, taken from [8], and a normal mass hierarchy.

Nowadays, short baseline reactor experiments detect $\bar{\nu}_e$ in Gd-doped liquid scintillator detectors, using the inverse beta decay (IBD) reaction on protons: $\bar{\nu}_e + p \to e^+ + n$. The IBD reaction signature is a time and space coincidence between the positron prompt and delayed gamma energy deposition, coming from neutron capture mostly on Gd ($E_\gamma \approx 8$ MeV) and H ($E_\gamma \approx 2.2$ MeV) nuclei. This rather unique signature offers a powerful background rejection. The prompt visible energy is made of the positron kinetic energy and the 2×0.511 MeV gamma rays resulting from its annihilation. This visible energy is related to the $\bar{\nu}_e$ energy by $E_{vis} \approx E_{\bar{\nu}_e} - 0.8$ MeV. The results presented in this article concern only $\bar{\nu}_e$ detected with a neutron capture on Gd nuclei. The time distribution between the prompt and delayed events follows an exponential law with a time constant corresponding to the neutron capture time on Gd nuclei, which is $\tau \sim 30\,\mu$s in DC.

2. The Double Chooz experiment

The Double Chooz experiment is 2-detector reactor $\bar{\nu}_e$ experiment located at the Chooz nuclear plant (France), which operates two pressurized water reactor cores, each delivering a 4.25 GW thermal power. The far detector (FD) has been running since 2011 and is located ~ 1050 m away from the reactor cores, with a rock overburden of 300 m.w.e. The near detector has recently finished been built and has been commissioned. It is located at an average distance of ~ 400 m from the two reactor cores and has a rock overburden of 120 m.w.e. It is identical to the FD, and will measure the reactor $\bar{\nu}_e$ flux with high precision, allowing cancellation of most of the reactor flux uncertainties in the measurement of θ_{13}.

The results presented here use data collected by the FD only, so that a precise reactor flux simulation was necessary to estimate the $\bar{\nu}_e$ rate and energy spectrum. Reactor $\bar{\nu}_e$ mostly originate from fission of ^{235}U, ^{239}Pu, ^{238}U and ^{241}Pu. Reactor flux predictions then rely on their respective fission

fractions within the reactor cores and $\bar{\nu}_e$ energy spectra. Fission fractions and their associated uncertainties are calculated using the MURE simulation code [10, 11], which has been benchmarked with another code [12]. MURE uses each reactor core instantaneous thermal power, location and composition of fuel elements as input data. These information are regularly provided by the Électricité de France company. The reference $\bar{\nu}_e$ spectra from ^{235}U, ^{239}Pu and ^{241}Pu are computed from a conversion of their associated β-spectrum measured at ILL [13, 14], while a recent measurement of the ^{238}U β-spectrum is used for the first time [15]. Additionally, the Bugey-4 $\bar{\nu}_e$ rate measurement performed at 15 m [16] is used to reduce the systematic uncertainty on the reactor flux normalization, after correcting for fuel composition differences in the Chooz and Bugey reactor cores. The systematic uncertainty on the IBD signal rate, coming from the reactor flux normalization, amounts to 1.7%. It would have been 2.8% without the use of the Bugey-4 rate measurement. The DC detector is a calorimetric scintillator detector made of four concentric cylindrical vessels. Figure 1 shows a schematic view of the DC detector. The innermost volume is the ν-target (NT). It is an 8-mm thick acrylic vessel filled with 10.3 m^3 liquid scintillator doped with Gd (1 g/L) to enhance capture of neutrons coming from IBD reactions. The γ-catcher (GC) surrounds the NT. It is a 55-cm thick layer of Gd-free liquid scintillator enclosed in a 12-mm thick acrylic vessel, and has been designed to maximize energy containment of the most energetic gamma rays coming from neutron captures in the NT. The GC is placed within the buffer volume, which is a 105-cm thick layer of mineral oil contained in a stainless steel tank, which has 390 low background 10-inch photomultiplier tubes (PMT). The buffer volume is primarily designed to shield the GC and NT volume from external radioactivity coming from the PMTs and surrounding materials. The detector sub-volumes described previously make the inner detector (ID). The outer detector (OD) is made of sub-volumes optically separated from the ID. The inner veto (IV) is a stainless steel tank enclosing the ID, and mounted by 78 8-inch PMTs. It is a 50-cm thick layer of liquid scintillator, and has been designed to veto cosmic ray muons crossing the detector. Further out is a 15-cm thick demagnetized steel shield protecting the detector from external gamma rays. An outer veto (OV) is placed on top of the detector, and consists of two aligned layers of plastic scintillator strips for the 2D reconstruction of vertical muons. An upper OV is also placed on top of the detector chimney, which is used for filling the different detector volumes and insertion of calibration sources (^{137}Cs, ^{68}Ge, ^{60}Co and ^{252}Cf and a laser). A multi-wavelength LED-fiber light injection system, mounted on the ID and IV PMTs, is also used periodically to calibrate the PMTs and readout electronics. Readout electronics are made of Front-End electronics (FEE) for PMT signal optimization, ahead of a Trigger system and flash-ADC electronics for ID and IV PMT signal digitization.

3. Data reduction

The dataset used for the analysis presented in this article corresponds to 467.90 days of live time (dead time corrected), collected from April 2011 to January 2013. The dataset totals 460.67 days where at least one of the two Chooz reactors is running (reactor-ON), while 7.24 days of data were collected when the two Chooz reactors were shut down (reactor-OFF).

3.1 Energy reconstruction

The DC collaboration pioneered the measurement of θ_{13} using the deformation of the recon-

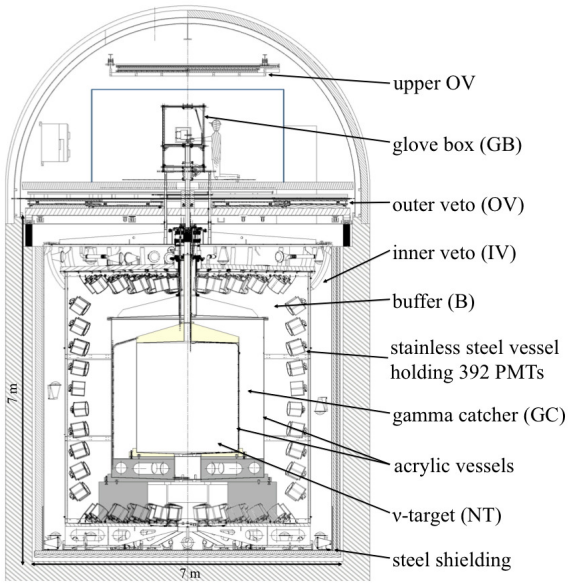

Figure 1: Double Chooz detector design.

structed $\bar{\nu}_e$ energy spectrum, thanks to a careful treatment of the energy reconstruction, which is applied both to recorded data and Monte Carlo (MC). A linearized photoelectron (PE) calibration procedure first converts raw integrated charges from each PMT channel into a number of PE, correcting for gain non-linearity. Each PE number is then corrected for the non-uniformity of the response over the full detection volume, by calculating response maps using spallation neutron captures on H for data and IBD neutron captures for MC. The absolute energy scale PE $\rightarrow$ MeV conversion factor is evaluated from the analysis of neutron captures on H using a ^{252}Cf source positioned at the detector center. A stability correction is also applied to the data to remove any remaining time variations, by looking and correcting for any changes in the H capture peak position reconstructed using spallation neutrons. The stability correction is cross-checked at different energies using the Gd capture peak position and α decays of ^{212}Po. Two further corrections are applied to the MC events to correct from non-linearities in the MC energy response relative to the data. The first correction arises from the modeling of the readout electronics and charge integration algorithm. The second comes from the scintillator modeling and is only applied to positrons. The total systematic uncertainty in the energy scale amounts to 0.74%.

3.2 Neutrino selection

Neutrino selection is done by applying different criteria. First, the minimum visible energy deposit the ID triggers on satisfies $E_{vis} > 0.4\,MeV$. The corresponding trigger efficiency is 100%. Events with $E_{vis} > 20\,MeV$ in the ID or $E_{vis} > 16\,MeV$ in the IV are rejected and tagged as muons, imposing a 1-ms veto to reject any muon-induced events. Light noise is a background caused by spontaneous light emission from some PMT bases. It is suppressed by requiring the selected events to satisfy the following criteria: i) q_{max} the maximum charge recorded by a PMT must be less or equal to 12% of the total charge corresponding to an event; ii) $1/N \times \sum_{i=0}^{N}(q_{max} - q_i)^2/q_i < 3 \times 10^4$ charge units, where N is the number of PMTs located less than 1 m away from the PMT with the

maximum charge; iii) $\sigma_t < 36\,\text{ns}$ or $\sigma_q > (464 - 8\sigma_t)$ charge units, where σ_t and σ_q are the standard deviation of PMT hit times and integrated charges, respectively. Event passing the previous selection criteria are used to search for IBD-like coincidences: the prompt and delayed visible energy must satisfy $0.5\,\text{MeV} < E_{vis} < 20\,\text{MeV}$ and $4\,\text{MeV} < E_{vis} < 10\,\text{MeV}$ respectively, with a correlation time in the [0.5 - 150] μs window and a distance between reconstructed prompt and delayed vertex less than 1 m. In addition, the delayed event must be the only one in a time window spanning 200 μs before and 600 μs after the prompt event.

3.3 Backgrounds

Accidental coincidences

Accidental background is random coincidences between 2 triggers satisfying the neutrino selection criteria. They mostly come from natural radioactivity in the materials making and surrounding the detector. Their random nature allows to study the accidental background rate and spectrum with a very good precision, by using multiple off-time coincidence windows placed at least 1 s after the prompt event. The accidental background rate is measured to be $0.0701 \pm 0.0003\,(\text{stat.}) \pm 0.026\,(\text{syst.})\,\text{d}^{-1}$.

Fast neutrons and stopping muons

Fast neutrons originate from spallation reactions of muons crossing the surrounding rocks. They can enter the detector and mimic the IBD signature by producing recoil protons (prompt) and be captured later (delayed). Stopping muons are muons which stop within the detector, giving a prompt signal, and subsequently decay producing Michel electrons, faking a delayed signal. Rejection of these backgrounds is achieved by discarding events fulfilling at least one of the following conditions: i) events with an OV trigger coincident with the prompt signal; ii) events with a delayed energy deposit inconsistent with a point-like vertex within the detector; iii) events for which the IV triggers (and would have then been rejected) and shows a correlated activity with the prompt signal within the detector. The last condition is used to extract the fast neutrons/stopping muons spectrum, which is found to be flat. The corresponding background rate in the neutrino candidate sample is estimated from an IBD-like coincidence search for which the prompt signal visible energy must be in the [20-30] MeV region. It amounts to $0.604 \pm 0.051\ \text{d}^{-1}$.

Cosmogenic isotopes

Unstable nuclei are produced by muon-induced spallation reactions within the detector. Spallation products such as ^{9}Li and ^{8}He have a decay mode where a neutron is emitted together with an electron and which is indistinguishable from an IBD reaction. The ^{9}Li and ^{8}He decay times are 257 ms and 172 ms, respectively, so that the 1-ms veto applied after a muon-tagged event is ineffective. A rejection criteria, based on a likelihood fit of the event distance to the muon track and of the number of neutron candidates following the muon in a 1-ms time window allows to reject 55% of ^{9}Li and ^{8}He cosmogenic background. The ^{9}Li/^{8}He contamination of the neutrino candidate sample is determined from fits to the time correlation between the IBD candidates and the previous muon. The rate of the remaining ^{9}Li/^{8}He background is estimated to be $0.97^{+0.41}_{-0.16}\,\text{d}^{-1}$. The events vetoed by the likelihood cut are used to build the ^{9}Li/^{8}He prompt energy spectrum (see inset in right panel of figure 2).

Source	Uncertainty (%)	[7]/[2]
Reactor flux	1.7	1.0
Detection efficiency	0.6	0.6
^{9}Li/^{8}He	+1.1/-0.4	0.5
Fast-n/stop-μ	0.1	0.2
Statitics	0.8	0.7
Total	+2.3/-2.0	0.8

Table 1: Signal and background normalization uncertainties, relative to signal prediction. [7]/[2] shows the improvement of the uncertainties with respect to [2].

4. Oscillation analyses

The neutrino selection criteria selected 17351 IBD candidates in the reactor-ON dataset. The expectation in the hypothesis of no-oscillation, including backgrounds, is 18290^{+370}_{-330}. In addition, 7 IBD candidates were observed in the 7.24 days reactor-OFF dataset. The prediction, including the residual neutrino emission after the two reactors are shut down, is $12.9^{+3.1}_{-1.4}$. The reactor-OFF dataset allows to test different (data driven) background estimates and adds constraints to the total background rate in the oscillation analysis. It is a unique advantage of DC, which has only two reactors. The normalization uncertainties on the signal and background predictions are summarized in table 1, showing also the improvement with respect to the previous analysis [2].

4.1 Reactor rate modulation analysis (RRM)

A correlation between the observed and predicted IBD candidate rates in different reactor conditions is expected. Therefore, a linear fit to the rate of observed rate as a function of expected rate of neutrino candidates in different reactor power bins allows to simultaneously determine $\sin^2(2\theta_{13})$ (proportional to the slope) and the total background rate (intercept) [6]. Treating the total background rate B = $1.64^{+0.41}_{-0.17}\,\mathrm{d}^{-1}$ as a nuisance parameter, the best fit ($\chi^2_{\mathrm{min}}/\mathrm{dof} = 4.2/6$) is found at $\sin^2(2\theta_{13}) = 0.090^{+0.034}_{-0.035}$ and B = $1.56^{+0.18}_{-0.16}\,\mathrm{d}^{-1}$ (see left panel of figure 2). A background model-independent measurement of θ_{13} is possible when B is treated as a free parameter. The best fit ($\chi^2_{\mathrm{min}}/\mathrm{dof} = 1.9/5$) corresponds to $\sin^2(2\theta_{13}) = 0.060 \pm 0.039$ and B = $0.93^{+0.43}_{-0.36}\,\mathrm{d}^{-1}$, and is consistent with the background-constrained fit. Finally, the impact of the reactor-OFF data has been studied by removing the reactor-OFF point (see left panel of figure 2). Keeping B unconstrained, the best fit ($\chi^2_{\mathrm{min}}/\mathrm{dof} = 1.3/4$) gives $\sin^2(2\theta_{13}) = 0.089 \pm 0.052$ and B = $1.56 \pm 0.86\,\mathrm{d}^{-1}$.

4.2 Rate + shape analysis

The rate + shape analysis extracts a value of θ_{13} by minimizing a χ^2 function in which the prompt energy spectrum of observed neutrino candidates is compared to a MC prediction in the no-oscillation hypothesis. A covariance matrix takes into account statistical and some systematic (reactor flux, MC normalization, ^{9}Li/^{8}He spectrum shape, accidental statistical) uncertainties in each bin and the bin-to-bin correlations. A set of nuisance parameters accounts for the other sources

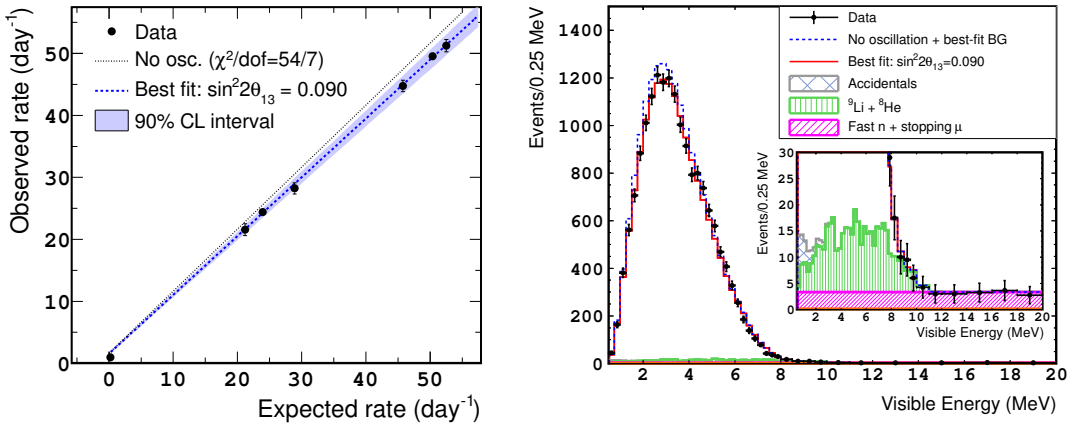

Figure 2: Left: Observed versus expected candidate daily rates for different reactor powers.The prediction under the null oscillation hypothesis (dotted line) and the best-fit with the background rate constrained by its uncertainty (blue dashed line) are shown. The first point corresponds to the reactor-OFF data. Right: Measured prompt energy spectrum (black points with statistical error bars), superimposed on the no-oscillation prediction (blue dashed line) and on the best fit (red solid line), with the stacked best-fit backgrounds added.

of uncertainty : Δm^2_{31}, the number of residual $\bar{\nu}_e$ when reactors are off (1.57 ± 0.47 events), the ^{9}Li/^{8}He and fast neutron/stopping muon rates, the systematic component of the uncertainty on the accidental background rate, and the energy scale. The best fit ($\chi^2_{\text{min}}/\text{dof} = 52.2/40$) is found at $\sin^2(2\theta_{13}) = 0.090^{+0.032}_{-0.029}$ (see left panel of figure 3).

In addition to the oscillation-induced deficit, a spectrum distortion is observed above 4 MeV (see left panel of figure 3). This distortion does not affect the measurement of θ_{13}. The excess above 4 MeV has been found to scale with reactor power, disfavoring a background origin. This structure is either consistent with an unaccounted reactor flux contribution and/or an unaccounted systematic uncertainty in the detector energy response. However, the RRM analysis performed in different energy bins favors a new reactor flux contribution [7].

Right panel of figure 3 shows the projected sensitivity of the rate + shape analysis of the DC 2-detector phase, using neutron captures on Gd. A precision of at least 15% on the measurement of $\sin^2(2\theta_{13})$ is expected after 3 years of data taking. A 0.2% relative detection efficiency is assumed, while the portion of uncorrelated reactor flux uncertainties is 0.1%. Backgrounds in the ND are estimated from measured backgrounds in the FD, accounting for differences in the muon flux. Comparing the expected sensitivity as shown in [2], the improvement is clear and is expected to increase further (for example, systematic uncertainties are limited by statistics).

5. Conclusion

The Double Chooz collaboration has recently finished the commissioning of the second detector. It is now operating in a 2 far and near detector mode. With a new dataset taken in a single-detector mode of 467.90 days of livetime, Double Chooz has achieved improved measurements of $\sin^2(2\theta_{13})$, using neutron captures on Gd. The most precise value is obtained from a fit to the observed positron energy spectrum: $\sin^2(2\theta_{13}) = 0.090^{+0.032}_{-0.029}$. A fully consistent result is found by

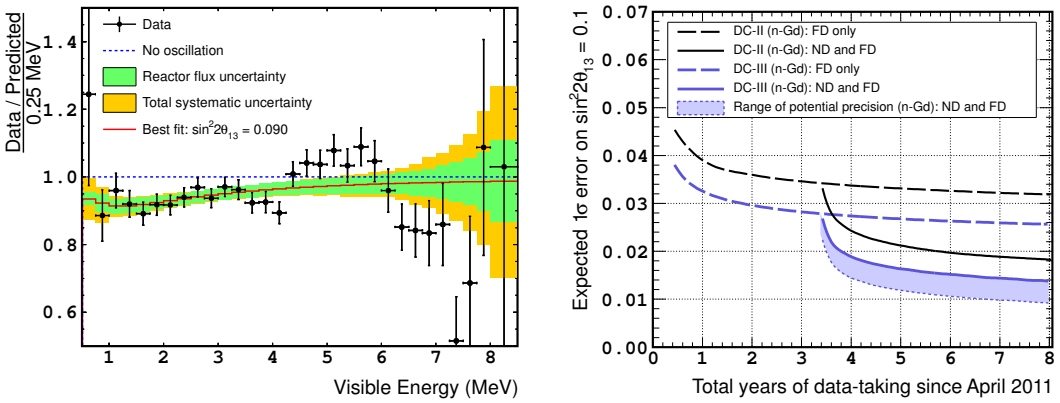

Figure 3: Left: Ratio of data to the no-oscillation prediction (black points) superimposed onto the best fit ratio (red solid line). The gold band represents the systematic uncertainty on the best-fit prediction. Right: DC projected sensitivity using IBD neutrons captured on Gd. The previous analysis, [2] with the FD only (black dashed line) and adding the ND (black solid line), and the current analysis, with the FD only (blue dashed line) and adding the ND (blue solid line), are shown. The shaded region represents the range of improvement expected by reducing the systematic uncertainty.

a fit to the observed neutrino candidate rate at different reactor powers: $\sin^2(2\theta_{13}) = 0.090^{+0.034}_{-0.035}$. An unexpected spectrum distortion has been observed above 4 MeV, with an excess correlated to the reactor power. It does not affect the measurement of $\sin^2(2\theta_{13})$.

References

[1] J. Beringer et al. (Particle Data Group), Phys. Rev. D86, 010001 (2012).

[2] Y. Abe et al. (Double Chooz collaboration), Phys. Rev. D86, 052008 (2012)

[3] F. P. An et al. (Daya Bay collaboration), Phys. Rev. Lett. 112, 061801 (2014)

[4] J. K. Ahn et al. (RENO collaboration), Phys. Rev. Lett. 108, 191802 (2012)

[5] Y. Abe et al. (Double Chooz collaboration), Phys. Lett. B723, 66 (2013)

[6] Y. Abe et al. (Double Chooz collaboration), Phys. Lett. B735, 51 (2014)

[7] Y. Abe et al. (Double Chooz collaboration), JHEP 10, 86 (2014)

[8] P. Adamson et al. (MINOS collaboration), Phys. Rev. Lett. 110, 171801 (2013)

[9] K. Abe et al. (T2K collaboration), Phys. Rev. Lett. 112, 061802 (2014)

[10] O. Meplan et al, in ENC 2015: European Nuclear Conference; nuclear power for the XXIst century: from basic research to high-tech industry (2005)

[11] NEA-1845/01, http://www.oecd-nea.org/tools/abstract/detail/nea-1845

[12] C. Jones et al., Phys. Rev. D 86, 012001 (2012)

[13] Th. A. Mueller et al., Phys. Rev. C 83, 054615 (2011)

[14] P. Huber et al., Phys. Rev. C 84, 024617 (2011)

[15] N. Haag et al., Phys. Rev. Lett. 122501(2014)

[16] Y. Declais et al. (Bugey-4 collaboration), Phys. Lett. B 338, 383 (1994)